International Journal of Applied Engineering Research ISSN 0973-4562 Volume 13, Number 10 (2018) pp. 7522-7528

Characterization of Voltage Rise Issue due to Distributed Solar PV Penetration

Abdullah T. Alshaikh, Thamer Alquthami, Sreerama Kumar R.

Department of Electrical and Computer Engineering, King Abdulaziz University, Jeddah-21589, Saudi Arabia.

Abstract

This paper discusses the voltage rise problem with high penetration of photovoltaic systems (PVS) on to the electric power grid. Conventional power grid are designed for the unidirectional power flow from generation to transmission then to distribution side where the loads are located. The reverse power flow caused by the high integration of distributed generation especially with low load conditions leads to certain technical challenges such as voltage rise, flicker, and frequency fluctuations. A typical distribution feeder is simulated with installed solar PVS to investigate the effect of grid connected distributed generators.

Keywords: Photovoltaic, Renewable, Solar, Voltage Rise, Distributed Generation

INTRODUCTION

Photovoltaic Systems (PVS) has been identified as a major alternative to the drastically and continuously increasing electric power demand all over the world. However, the integration of solar power generation with the electric grid comes with technical issues. The conventional electric power networks are designed to operate with unidirectional power flow from generation through transmission and distribution systems to the load end. On the other hand, with the installation of photovoltaic distributed generation (PV-DG), the power generated in excess of the local load demand can be injected into the power grid, leading to reverse power flow from load end. This may lead to major challenges such as feeder voltage rise and its rapid fluctuations. This paper reviews the voltage rise issues with the increasing high PVS installations on a distribution feeder. Backward / Forward sweep power flow analysis is applied on the IEEE 13 node test feeder with and without PVS to show the impact of voltage rise.

LITERATURE REVIEW

Katiraei, F. *at el.* have introduced a new study tools and methodologies to help utility engineers to investigate the impact of PV-DG [1]. They have discussed the following most common impacts of PV-DG:

i. Reverse power flow, which may affect protection coordination and line voltage regulators.

ii. Voltage profiles changes, including voltage rise more than 0.03 p.u.

iii. Interaction with the capacitor banks, LTCs, and line voltage regulators, which may cause frequent operation of these devices.

iv. Reactive power fluctuations due to frequent capacitor bank switching.

v. Expected changes in feeder section loading, which may cause component overloading.

Many studies have been presented to address these issues. One major issue is the voltage rise due to high level of PV penetration [2-4]. In [2], Teleke S. *et al.* have discussed the impact of photovoltaic distribution generation on the quality and reliability of the power network. A model has been simulated and shown that PV-DG can cause feeder over voltage, which may lead to increase in the operation of the transformer tap-changer. A simulation study has identified that with only 20 % of PV feeder penetration, tap changer operates excessively to cope with voltage fluctuation [3]. This could potentially reduce the life expectancy of load tap changers (LTCs).

In Ref. [4], Masoum *et al.* have addressed the impact of rooftop PVs on voltage profile. The study shows that there is an improvement on voltage profile and transformer loading but there will be a voltage rise with high penetration of PVs, especially during off peak times when the load is generally at a low level. In terms of a large scale solar PV implementation, Hsieh *et al.* have studied the impact of such a large system on the power grid in [5], where a large scale PV system has been installed in a sporting stadium connected to a power network for the investigation of the voltage variation and power losses of distribution feeders. Power flow analysis has been performed to show the impact of integrating PV generation system. The simulation results has shown that the system voltage has been improved during the day time. It was found that voltage drop can be minimized. After installing the PV system, there was reduction in daily power loss.

Liu, Y. *et al.* [6] have found that the voltage rise due to high PV penetration may increase the voltage to exceed the voltage boundary standard limits as specified by ANSI C84.1 [7]. In [6], of PV penetration. The study shows that the PV inverters were over-rated allowing significant reactive power capability during full rated PV output. It also shows that PV inverter can provide voltage support and hence reduced the need of the capacitors. Finally, it was concluded that the distribution fleet of PV system can be controlled to ensure that the feeder can provide its fair share of reactive power.

Tonkoski *et al.* in [8] have proposed a methodology to prevent overvoltage condition caused by high level of PV integration. The methodology proposed is to limit the injecting capacity of

the PV system to a conservative value by applying droop-based active power curtailment techniques. They found that this technique is attractive because it requires minor modification in inverter control logic. It is the same technique used for power sharing among several generators connected in parallel. In addition, the system can only be activated when there is a need to minimize the amount of curtailed active power. To simulate the proposed methodology, two typical schemes have been presented. The first scheme was set to have the same droop coefficients for all the inverters in the system, while the other scheme was having different set of droop coefficients for the inverters in the system. The study found that for the first scheme, the contribution required from each inverter to prevent over voltage were different. The study also has shown that the feeder downstream inverter is required to curtail more power than the others. This set up is seen to be more expensive than the active power curtailment scheme. A voltage control algorithm has been presented in [9] and used also in [10]. Tang, Ye, *et al.* in [11] have studied the impact of PV injection for different capacities, locations, and operation modes.

Liu, Xiaohu, *et al.* have proposed a method to solve the voltage rise due to large PV penetration. [12]. In this approach, OLTC is assumed to work on a conventional network with unidirectional power flows. Therefore, more installations of distribution generation units causes higher stress on tap changers. The proposed controller relieves the stress on tap changer, shave the distribution network peak load, and decrease the power losses on the transmission and distribution networks due to large PV penetration. Ref. [19] also has investigated the effect of installation of solar PV and battery system in a practical distribution network. Ref. [12] has proposed an automated distribution control approach to guarantee that generator injections alone do not cause significant voltage rise.

Tonkoski, *el al.* in [13] has investigated the impact of high PV penetration on the voltage profile in residential neighborhoods. Several cases have been studied to investigate the maximum limit of PV penetration and maximum power allowed to guarantee that the voltage will be at adequate levels.

The following section gives an overview load flow algorithm and the simulation results of a standard distribution feeder with integrated PV system.

ALGORITHM FOR LOAD FLOW ANALYSIS OF DISTRIBUTION FEEDERS.

The conventional load flow methods such as Gauss Seidel method and Newton-Raphson method of load flow analysis, which are very effectively used for transmission networks, are not suitable for the load flow analysis of distribution networks. This is mainly because of the radial structure of the distribution network and high R/X ratios. Backward/forward sweep method is used in this work for the load flow analysis of radial distribution network. This method involves first numbering the nodes in ascending order from layer to layer to identify the path from the root node to the terminal node. Backward/forward sweep method is an iterative method based on two set of recursive equations, the first set is to calculate the power flow through the brunches starting from last node and moving in backward direction to the source or root node. The other set is to calculate the voltages of each node starting from the source node and moving forward direction to the last node. Thus, in the forward sweep, the voltage drop calculation is performed with power flow updated. It starts from the source node to the last node to calculate the voltages at each node. Backward sweep is power flow solution with bus voltages updated. It starts from the last node to the source node to update the power flow results with the new value of voltages obtained from the forward path [14-17]. With reference to Figure 1, the equations used in backward sweep are:

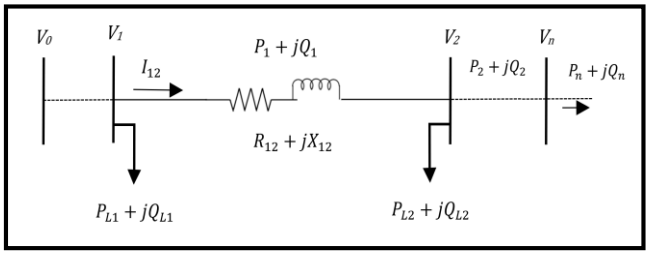

Figure. 1. Simplified radial distribution network

$$P_1 = P_2 + P_{L2} + R_{12} \times \frac{P_2'^2 + Q_2'^2}{|V_2|^2} \quad (3.1)$$

$$Q_1 = Q_2 + Q_{L2} + X_{12} \times \frac{P_2'^2 + Q_2'^2}{|V_2|^2} \quad (3.2)$$

Where $P_2'^2 = P_2 + P_{L2}$ and $Q_2'^2 = Q_2 + Q_{L2}$

P_{L2} *and* Q_{L2} *are the load connected at bus no.* 2

P_2 *and* Q_2 *are active and reactive power at bus no.* 2

If distributed PVS are connected to the grid, it can be treated as negative PQ load. In this case, the total P_{L2} and Q_{L2} are

$$P_{L2} = P_{Load} - P_{PV} \quad (3.3)$$

$$Q_{L2} = Q_{Load} - Q_{PV} \quad (3.4)$$

With reference to Figure 1, the equations used in forward sweep are

$$I_{12} = \frac{V_1 \angle \delta_1 - V_2 \angle \delta_2}{R_{12} + jX_{12}} \quad (3.5)$$

$$I_{12} = \frac{P_1 + jQ_1}{V_1 \angle -\delta_1} \quad (3.6)$$

From equations 3.5 and 3.6, one obtains

$$\frac{P_1 + jQ_1}{V_1 \angle -\delta_1} = \frac{V_1 \angle \delta_1 - V_2 \angle \delta_2}{R_{12} + jX_{12}} \quad (3.7)$$

$$V_1^2 - V_1V_2\angle(\delta_2 - \delta_1) = (P_1 - jQ_1)(R_{12} + jX_{12}) \quad (3.8)$$

Separating the real part and imaginary part from equation 3.8, one obtains

$$V_1V_2\cos(\delta_2 - \delta_1) = V_1^2 - (P_1R_{12} + Q_1X_{12}) \quad (3.9)$$

$$V_1V_2\sin(\delta_2 - \delta_1) = Q_1R_{12} - P_1X_{12} \quad (3.10)$$

Squaring and adding equations 3.9 and 3.10, equations (3.11), (3.12), and (3.13) respectively becomes:

$$(V_1V_2)^2 = [V_1^2 - (P_1R_{12} + Q_1X_{12})]^2 + [Q_1R_{12} - P_1X_{12}]^2$$

$$(V_1V_2)^2 = V_1^4 - 2V_1^2(P_1R_{12} + Q_1X_{12}) + (R_{12}^2 + X_{12}^2)(P_1^2 + Q_1^2)$$

$$V_2 = \sqrt{V_1^2 - 2(P_1R_{12} + Q_1X_{12}) + (R_{12}^2 + X_{12}^2)\frac{(P_1^2+Q_1^2)}{V_1^2}}$$

The algorithm for the Forward/Backward Sweep Approach for the load flow analysis of distribution network utilizing these equations is given in Figure 2.

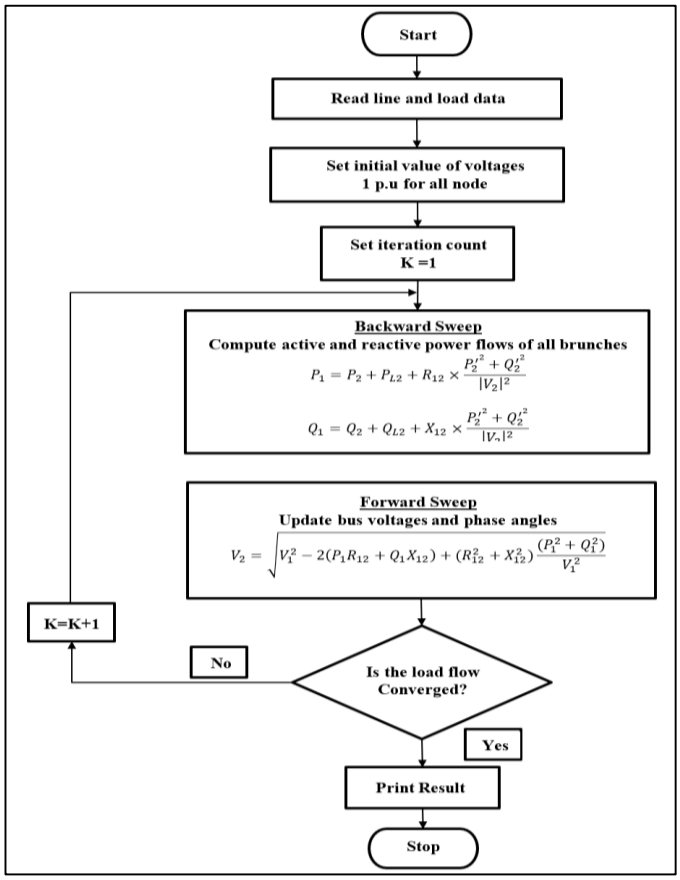

Figure 2. Algorithm of Forward/Backward sweep method

For three phase systems, the backward equation is

$$S_n^{a,b,c} = S_i^{a,b,c} + Loss_n + \sum_{m\in M} S_m^{a,b,c} \quad (3.14)$$

a, b, c	Refer to phases
S_n	The power of brunch n
S_i	The absorbed power by the connected load at the ending node of brunch n
$Loss_n$	Power loss of brunch n
M	Set of brunches which are connected to the ending node of brunch n
S_m	The power of brunch m

The forward equation is given by

$$I_n^{a,b,c} = \left(\frac{S_n^{a,b,c}}{V_j^{a,b,c}}\right)^* \quad (3.15)$$

Where I_n is the current in the branch n, and j is the sending node of branch n

$$V_i^{a,b,c} = V_j^{a,b,c} - Z_n^{a,b,c} \times I_n^{a,b,c} \quad (3.16)$$

$$Loss_{n,abc} = \left(V_j^{a,b,c} - V_i^{a,b,c}\right) \cdot I_n^{a,b,c} \quad (3.17)$$

TEST FEEDER DATA AND SIMULATION RESULTS

The single line diagram of the 13-node 4.16 kV test feeder is shown in Figure 3. The feeder data are given in [18].

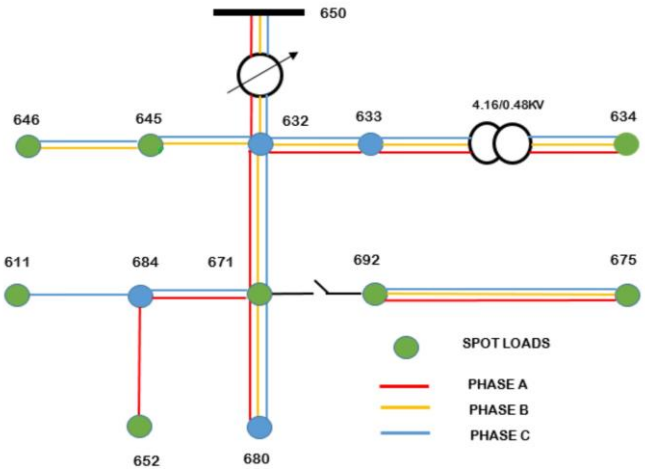

Figure 3. Single Line Diagram of 13 node test feeder

The results of load flow analysis of the feeder without any PVS installation is shown in Figure 4, Table 1, Table 2 and Table 3 respectively. The results are obtained for the system without considering PV system. From the results, it can be observed that there is voltage rise in the line from the source to node 632. Further, an over-load occurs from node 675 to the line where the

shunt capacitor is located.

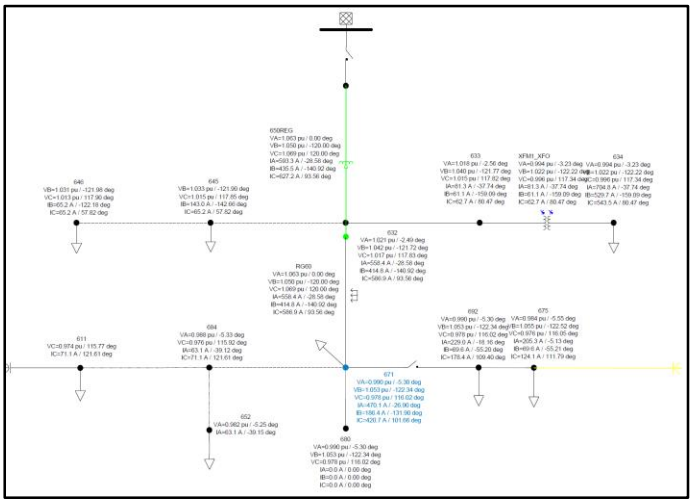

Figure 4. Load flow results of the 13 node test feeder without PV system

Table 1: Power flow results of 13 node feeder without PVS

Total Summary	KW	KVAR
Sources	3577.30	1725.94
Load Demand	3466.00	2102.00
Shunt capacitors	0.00	-701.42
Line Capacitance	0.00	-0.39
Line Losses	105.77	316.31
Transformer Losses	5.44	9.89
Total Losses	111.21	326.20

Table 2: Overload conditions of 13 node feeder without PVS

Abnormal Conditions	Phase	Worst Condition in Line	Value (%)
Overload	A	from 675 to Capacitor	96.77
	B	from 675 to Capacitor	111.33
	C	from 675 to Capacitor	95.20

Table 3: Over-Voltage conditions of 13 node feeder without PVS

Abnormal Conditions	Phase	Worst Condition at Node	Value (%)
Over-Voltage	A	RG60	106.25
	B	675	105.52
	C	RG60	106.88

The voltage profile can be shown from the source to any node. The voltage profile at node 632 is within limits as shown in Figure 5. Figure 6 shows the voltage profile traced from the source through the 605 meters long 3-phase line till node 632. After that, the line from node 632 to 646 get power supplies from phase B and phase C only. However, the voltage profile is within limits. The voltage profile at node 671, as shown in Figure 7, indicate that the node voltage is always within limits. However, phase B rises to a value near to its maximum limits. This is because the line from node 671 to 684 gets the power from phase A and phase C only. The voltage profile at node 692 as shown in Figure 8 is within its limits. The voltage profile at node 675 shown in Figure 9 indicates that the phase-B voltage is very near to its maximum limit as compared to the other phases. This is mainly because this phase is operating at lightly loaded condition.

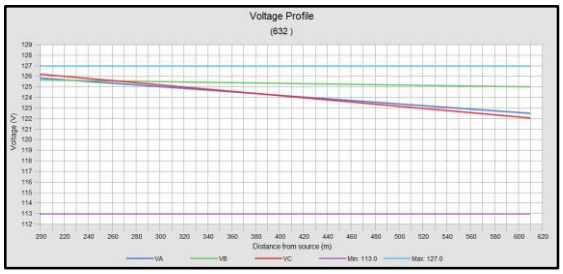

Figure 5. Voltage profile of node 632

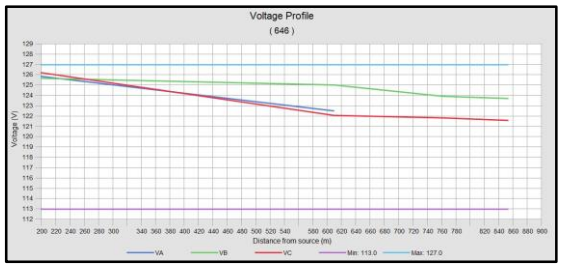

Figure 6. Voltage profile of node 646

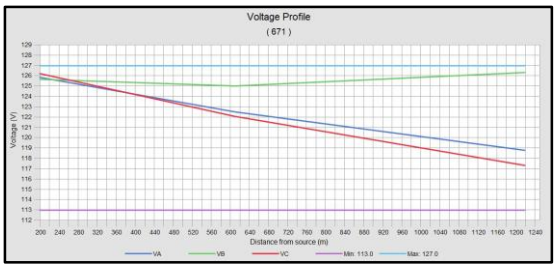

Figure 7. Voltage profile of node 671

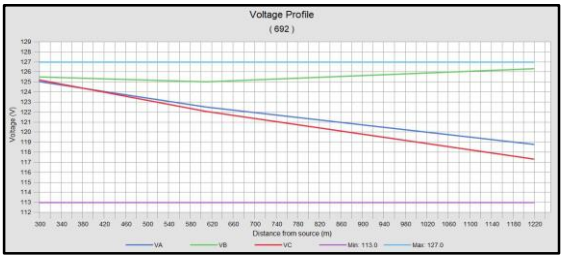

Figure 8. Voltage profile of node 692

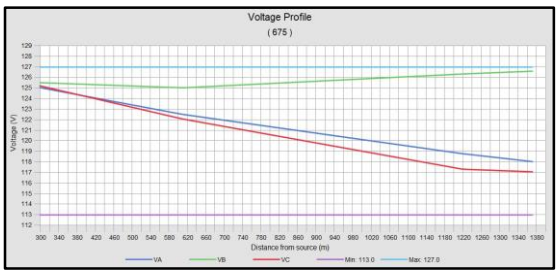

Figure 9. Voltage profile of node 675

Assuming PVS installation at each of the identified nodes as given in Table 4, the power flow analysis is repeated. Based on Ref. [18], The loads at node 646, 671, 692, and 675 and the proposed PVS installations are shown in Table 4. The corresponding simulation results are shown in Figure.10.

Table 4: The loads and PV injection of the proposed node

Node	Load	Ph-AB		Ph-BC		Ph-CA		PV Injection	
		Ph-A		Ph-B		Ph-C			
	Configuration	kW	kVar	kW	kVar	kW	kVar	kW*	Ph
646	Δ	0	0	230	132	0	0	161	BC
671	Δ	385	220	385	220	385	220	808	ABC
692	Δ	0	0	0	0	170	151	119	AC
675	Y	485	190	68	60	290	212	590	ABC

*70% of total load at each node has taken.

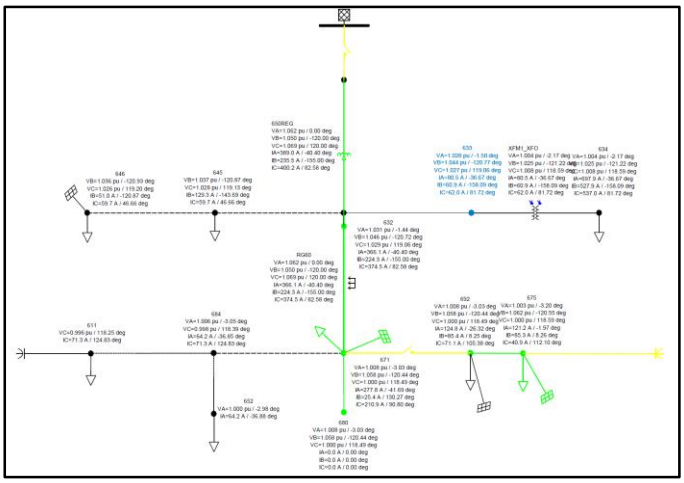

Figure 10. Load flow results of 13 node test feeder with PVS Installations

A comparison of the results of voltages profile given in Figures 5 to 9 with those given in Figure 11 to 15 indicates the following observations:

The voltage profile is slightly increased at node 632 and 646 after the installation of PV module as shown in Figure 11 and Figure 12. However, the voltage profile at these nodes are within the allowable limits. The voltage profile of phase B increases to the maximum limit at node 671, 692 and 675 after the installation of PV module as shown in Figure 13, Figure 14 and Figure 15 respectively.

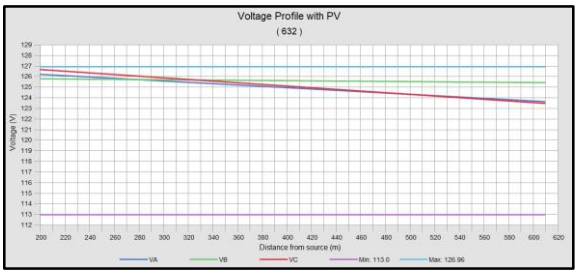

Figure 11. Voltage profile of node 632 of the test feeder with PVS

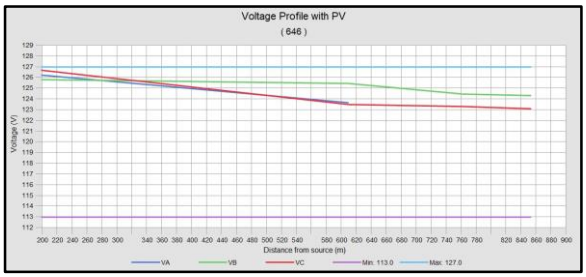

Figure 12. Voltage profile of node 646 of the test feeder with PVS

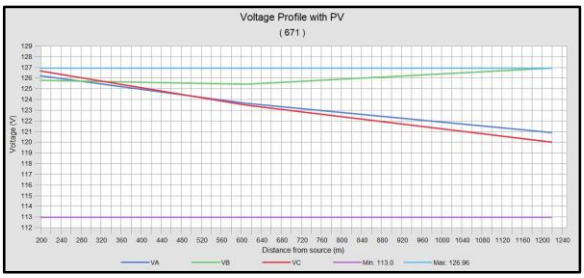

Figure 13. Voltage profile of node 671 of the test feeder with PVS

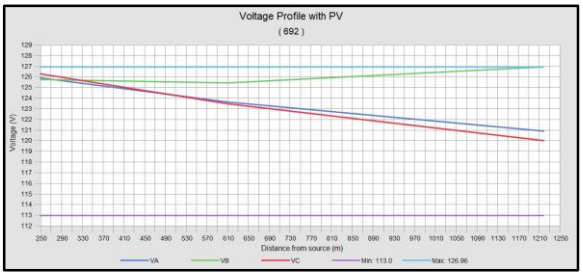

Figure 14. Voltage profile of node 692 of the test feeder with PVS

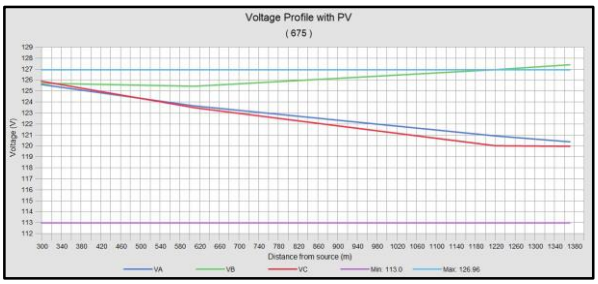

Figure 15. Voltage profile of node 675 of the test feeder with PVS

CONCLUSION

This paper has reviewed the research and developments related to the various issues, particularly the voltage rise problem due to the high level of PVS installations in a distribution system. The literature review indicates that the high level of PV integration comes with technical issues such as reverse power flow, voltage profiles changes, reactive power fluctuations, changes in feeder section loading, and Interaction with regulator devices such as LTCs, and line VRs. Voltage rise is one of the major issues that has to be minimized in order to reduce the unfavorable impact of high level of PV penetration. Significant research has been carried out to investigate this impact and several mitigation measures have also been proposed.

ACKNOWLEDGMENT

This Project was funded by the Deanship of Scientific Research (DSR), at King Abdulaziz University, Jeddah, under grant no.G-135-562-38. The authors, therefore, acknowledge with thanks DSR for technical and financial support.

REFERENCES

[1] Katiraei, F. and J.R. Agüero, Solar PV integration challenges. Power and Energy Magazine, IEEE, 2011. 9(3): p. 62-71.

[2] Teleke, S., et al. Analysis of interconnection of photovoltaic distributed generation. in Industry Applications Society Annual Meeting (IAS), 2011 IEEE. 2011. IEEE.

[3] Ari, G. and Y. Baghzouz. Impact of high PV penetration on voltage regulation in electrical distribution systems. in Clean Electrical Power (ICCEP), 2011 International Conference on. 2011. IEEE.

[4] Masoum, A.S., et al. Impact of rooftop PV generation on distribution transformer and voltage profile of residential and commercial networks. in Innovative Smart Grid Technologies (ISGT), 2012 IEEE PES. 2012. IEEE.

[5] Hsieh, W.-L., et al., Impact of PV generation to voltage variation and power losses of distribution systems. Electric Utility Deregulation and Restructuring and Power Technologies (DRPT), 2011 4th International Conference on. IEEE, 2011.

[6] Liu, Y., et al. , Distribution system voltage performance analysis for high-penetration PV. Energy 2030 Conference, 2008. ENERGY 2008. IEEE., 2008.

[7] Standard, A., C84. 1-1982. American National Standard for Electric Power System and Equipment–Voltage Ratings (60Hz).

[8] Tonkoski, R., Luiz AC Lopes, and Tarek HM El-Fouly. , Coordinated active power curtailment of grid connected PV inverters for overvoltage prevention. Sustainable Energy, IEEE Transactions on 2.2, 2011: p. 139-147.

[9] Bollen, M. and A. Sannino, Voltage control with inverter-based distributed generation. IEEE transactions on Power Delivery, 2005. 20(1): p. 519-520.

[10] Vasquez, J.C., et al., Voltage support provided by a droop-controlled multifunctional inverter. Industrial Electronics, IEEE Transactions on, 2009. 56(11): p. 4510-4519.

[11] Tang, Y., et al. , Assessment of medium voltage distribution feeders under high penetration of PV generation. Control and Modeling for Power Electronics (COMPEL), 2015 IEEE 16th Workshop on. IEEE, 2015., 2015.

[12] Liu, X., et al. , Coordinated control of distributed energy storage system with tap changer transformers for voltage rise mitigation under high photovoltaic penetration. Smart Grid, IEEE Transactions on 3.2, 2012: p. 897-906.

[13] Tonkoski, R., Dave Turcotte, and Tarek HM El-Fouly,

Impact of high PV penetration on voltage profiles in residential neighborhoods. Sustainable Energy, IEEE Transactions on 3.3 2012: p. 518-527.

[14] Sunisith, S. and K. Meena, Backward/Forward sweep based distribution load flow method. International Electrical Engineering Journal (IEEJ), 2014. 5(9).

[15] Rupa, J.M. and S. Ganesh, Power flow analysis for radial distribution system using backward/forward sweep method. International Journal of Electrical, Computer, Electronics and Communication Engineering, 2014. 8(10): p. 1540-1544.

[16] Eminoglu, U. and M.H. Hocaoglu, Distribution systems forward/backward sweep-based power flow algorithms: a review and comparison study. Electric Power Components and Systems, 2008. 37(1): p. 91-110.

[17] Muruganantham, B., R. Gnanadass, and N. Padhy. Unbalanced load flow analysis for distribution network with solar pv integration. in Power Systems Conference (NPSC), 2016 National. 2016. IEEE.

[18] Kersting, W.H. Radial distribution test feeders. in Power Engineering Society Winter Meeting, 2001. IEEE. 2001. IEEE.

APPENDIX

Table A.1. Underground line configuration data

Config.	Phasing	Cable	Neutral	Space ID
606	A B C N	250,000 AA, CN	None	515
607	A N	1/0 AA, TS	1/0 Cu	520

Table A.2. Overhead line configuration data

Config.	Phasing	Phase	Neutral	Spacing
		ACSR	ACSR	ID
601	B A C N	556,500 26/7	4/0 6/1	500
602	C A B N	4/0 6/1	4/0 6/1	500
603	C B N	1/0	1/0	505
604	A C N	1/0	1/0	505
605	C N	1/0	1/0	510

Table A.3. Line segment data

Node A	Node B	Length(ft.)	Config.
632	645	500	603
632	633	500	602
633	634	0	XFM-1
645	646	300	603
650	632	2000	601
684	652	800	607
632	671	2000	601
671	684	300	604
671	680	1000	601
671	692	0	Switch
684	611	300	605
692	675	500	606

Table A.4. Capacitor data

Node	Ph-A	Ph-B	Ph-C
	kVAr	kVAr	kVAr
675	200	200	200
611			100
Total	200	200	300

Table A.5. Regulator data

Regulator ID:	1		
Line Segment:	650 - 632		
Location:	650		
Phases:	A - B -C		
Connection:	3-Ph,LG		
Monitoring Phase:	A-B-C		
Bandwidth:	2.0 volts		
PT Ratio:	20		
Primary CT Rating:	700		
Compensator Settings:	Ph-A	Ph-B	Ph-C
R - Setting:	3	3	3
X - Setting:	9	9	9
Volltage Level:	122	122	122

Table A.6. Transformer data

	kVA	kV-high	kV-low	R - %	X - %
Substation:	5,000	115 - D	4.16 Gr. Y	1	8
XFM -1	500	4.16 – Gr.W	0.48 – Gr.W	1.1	2

Table A.7. Spot load data

Node	Load	Ph-A	Ph-A	Ph-B	Ph-B	Ph-C	Ph-C
	Model	kW	kVAr	kW	kVAr	kW	kVAr
634	Wye - Constant kW and kVAr	160	110	120	90	120	90
645	Wye - Constant kW and kVAr	0	0	170	125	0	0
646	Delta - Constant Impedance	0	0	230	132	0	0
652	Wye - Constant Impedance	128	86	0	0	0	0
671	Delta - Constant kW and kVAr	385	220	385	220	385	220
675	Wye - Constant kW and kVAr	485	190	68	60	290	212
692	Delta - Constant Current	0	0	0	0	170	151
611	Wye - Constant Current	0	0	0	0	170	80
	TOTAL	1158	606	973	627	1135	753

Table A.8. Distributed Load Data

Node A	Node B	Load	Ph-A	Ph-A	Ph-B	Ph-B	Ph-C	Ph-C
		Model	kW	kVAr	kW	kVAr	kW	kVAr
632	671	Y-PQ	17	10	66	38	117	68